

Mono- and double-mutant mouse models of Parkinson's disease display severe mitochondrial damage

Christine C. Stichel^{1,*}, Xin-Ran Zhu^{2,†}, Verian Bader^{2,†}, Bettina Linnartz², Saskia Schmidt² and Hermann Lübbert^{2,3}

¹Biofrontera Bioscience GmbH, D-51377 Leverkusen, Germany, ²Department of Animal Physiology, Ruhr-University of Bochum, D-44780 Bochum, Germany and ³Biofrontera AG, D-51377 Leverkusen, Germany

Received December 27, 2006; Revised February 7, 2007; Accepted March 26, 2007

Mutations in the gene encoding α -synuclein (asyn) causes autosomal-dominant, in the parkin gene autosomal-recessive forms of Parkinson's disease (PD). The pathophysiology of PD is poorly understood, even though published evidence suggests a role for mitochondria in the pathogenesis. To gain insight into the influence of asyn and parkin on mitochondrial integrity and function, we have generated several mono-mutant mouse lines expressing doubly mutated human asyn (hm²asyn) under the control of two different promoters, or a targeted deletion of Parkin (Parkin-Exon3-knockout). Both mouse lines were crossed to generate the double-mutant. Here we compare the ultrastructure and functional properties of mitochondria in the substantia nigra (SN), the striatum, the cerebral cortex (Cx) and skeletal muscle of young (2–3 months) and aged (12–14 months) mono- and double-mutants mice. We observed severe genotype-, age- and region-dependent morphological alterations of mitochondria in neuronal somata. The number of structurally altered mitochondria was significantly increased in the SN of both double-mutants and in the Cx of one mono- and one double-mutant line. These alterations coincided with a reduced complex I capacity in the SN, but were neither accompanied by alterations in the number or the size of the mitochondria nor by leakage of cytochrome *c*, Smac/DIABLO or Omi/HtrA2. None of the transgenic animals developed any gross histopathological abnormalities or overt motor disabilities. Together our results provide compelling evidence that (i) both, asyn and parkin are relevant for mitochondrial integrity, (ii) the influence of these proteins on mitochondria are age- and tissue-specific and (iii) changes of mitochondrial morphology do not inevitably cause functional impairments.

INTRODUCTION

Parkinson's disease (PD) is the most common movement disorder and the second most prevalent neurodegenerative disease. The majority of cases of PD appear to be sporadic in nature and familial PD with specific genetic defects accounts for fewer than 10% of all cases of PD. In recent years, mutations or polymorphisms in 10 genes (α -synuclein, parkin, UCHL1, DJ-1, LRRK2, NR4A2, Pink1, HTRA2, tau, ATP13A2) have been identified in PD families (1; reviewed in 2–4), and five other loci across the genome harbour as yet unidentified

genes (5). The clinical manifestations of PD include resting tremor, muscular rigidity, bradykinesia and postural instability. These severe symptoms are caused by a progressive degeneration of dopaminergic neurons. The accumulation of proteinaceous cytoplasmic inclusions known as Lewy bodies is another pathological hallmark of PD; however, it is absent in some familiar forms of PD (6,7). The aetiology of PD is still unknown, but previous work suggests that oxidative stress, inflammation, aberrant protein degradation and, in particular, mitochondrial dysfunction may be involved in the PD-associated neuronal degeneration (reviewed in 8–11).

*To whom correspondence should be addressed at: Animal Physiology, Biology, ND5/132 Ruhr-University Bochum, D-44780 Bochum, Germany. Tel: +49 2343225829; Fax: +49 2343214189; Email: c.stichel-gunkel@biofrontera.com

†The authors wish it to be known that, in their opinion, the first 3 authors should be regarded as joint First Authors.

The latter, impairment of mitochondrial function, is emerging as a common theme in PD pathogenesis. Whether it plays a causative role in PD has not yet been elucidated, but several studies suggest that deficiencies in mitochondrial function are involved in the degeneration of dopaminergic neurons. Evidence for a connection between mitochondria and PD stems from the observation that a defect in the activity of respiratory chain protein complex I was identified in the substantia nigra (SN) (12), the striatum (ST) (13), the frontal cortex (Cx) (14), platelets (15) and in leukocytes (16) of PD patients. This link was further strengthened when (i) a mitochondrial localization of DJ-1, Pink1, HTRA2 and parkin (17–21), (ii) the interaction of Pink1 and parkin in the regulation of mitochondrial function (20,22) and (iii) the phenotype of some transgenic mice carrying PD-inducing human gene mutations were reported. In transgenic mice overexpressing mutant α -synuclein (synTG) and in DJ1-(DJ1-KO), HTRA2- (HTRA2-KO) and parkin-null mice (PaKO) an increased susceptibility to mitochondrial toxins (21,23–26) was noted. For both, synTG and PaKO mice, reductions in respiratory capacity were described (27–29). Proteins related to energy metabolism were found to be differentially expressed (30,31). Although these data suggest that most of the PD-related mutations converge on mitochondrial pathways, morphological signs of mitochondrial defects, such as those seen in the mesencephalon and skeletal muscle of PD patients (32–35), were only observed in brain motor regions of one synTG line (28). PaKO mice were reported to have deficiencies in mitochondrial function, but lacked gross morphological abnormalities (29). In contrast, *Drosophila* models of PD displayed severe histopathological mitochondrial changes, which were restricted to flight muscle and spermatids. In the flies, loss of Pink1 (20,22,36) or parkin (37) leads to enlarged and disintegrated mitochondria.

An explanation for the lack of a mitochondrial phenotype in previous publications of such transgenic mice was hindered by genetic differences between the mouse strains used to generate the transgenics. All transgenics analysed in previous studies were of the F1 generation with a 50:50% background. The disparity between human patients and mouse models might also be caused by an age effect. PD is a disorder with late onset and up to date most analysed transgenics were of young ages.

To address these issues, we provide a detailed comparative, ultrastructural analysis of neuronal morphology, with emphasis on mitochondrial integrity, in three different brain regions and skeletal muscle of various young (3 months) and aged (12–14 months) transgenics mice of the F4 generation of mice carrying Parkinson mutations. Moreover, we addressed the question whether changes in mitochondrial structure are accompanied by dysfunctions in respiration or enhanced release of intermembrane space proteins. In addition to two monogenic lines, synTG with a pure C57BL/6 background and the F4 generation of PaKO, we generated and analysed double-mutant animals carrying both α -synuclein mutations and the parkin knock-out, to unravel synergies and/or an interactions of these proteins in pathways leading to mitochondrial defects.

Preliminary results of the study were presented in abstract form (38).

RESULTS

Transgenic mouse generation

Targeted deletion of parkin exon 3 results in a frameshift after amino acid 57 of parkin. A loss of exon 3 has also been observed in humans, leading to a very early form of PD (39). An RT-PCR analysis of total RNA isolated from the brains of wild-type mice and PaKO siblings using a primer pair specific for exons 1–6 showed a shorter parkin transcript in homozygous PaKO than in wild-type mice (Fig. 1A). Sequencing the PCR fragments confirmed that the deletion of exon 3 causes an abnormal splicing from exon 2 directly onto exon 4 (data not shown). Lack of full-length parkin protein in homozygous PaKO and a reduced level in heterozygous PaKO mice was demonstrated by western blotting of total brain protein with a polyclonal antibody against the N-terminal part of mouse parkin (Fig. 1B). The truncated C-terminus of the parkin protein was not detected.

Both α -synuclein transgenic lines, BA(β -actin)syn and TH(tyrosine hydroxylase)syn, expressed the transgene in a promoter-dependent fashion. Radioactive western blot analysis (Fig. 1C and D) and immunohistochemistry (40) revealed an up to 8-fold stronger transgene expression in the BA syn mice compared with the TH syn mice. This expression difference depended on the brain region and mirrored the difference between BA- and TH-promoter activities in the adult mouse. All α -synuclein transgenic lines exhibited neuronal expression of the transgene, but with a different regional and cellular distribution (40).

Disruption of the Parkin gene in double-mutants (BA syn/PaKO, TH syn/PaKO) neither affected the α -synuclein transgene expression level (Fig. 1C and D) nor its spatial expression pattern (data not shown).

General health and histopathology of transgenic lines

All transgenic lines (mono- and double-mutants) were viable, fertile and did not display any gross pathological abnormalities. The brain and the spinal cord appeared macroscopically normal. To assess whether the gene mutations induced histopathological changes in the nigro-striatal dopaminergic system, we applied immunohistochemical and histological methods to study the morphology of the dopaminergic system, the occurrence of cell death and the formation of astro- and microgliosis. None of the lines displayed morphological or quantitative changes of dopaminergic neurons and axons [data shown for double-mutants versus littermates (LM, Fig. 2A–F), cell death or micro- (data shown for double-mutants versus LM, Fig. 2G–I) and astrogliosis (data shown for double-mutants versus LM, Fig. 2J–L) in the SN, the ST, the locus coeruleus and the cerebral cortex (Cx)].

Ultrastructural abnormalities in neurons of old transgenic mice (12–14 months)

Electron microscopy was used to examine ultrastructural changes in the SN, the ST and the Cx of both, mono- and double-mutant animals. In this study, we concentrated on changes in neuronal somata and disregarded those present in

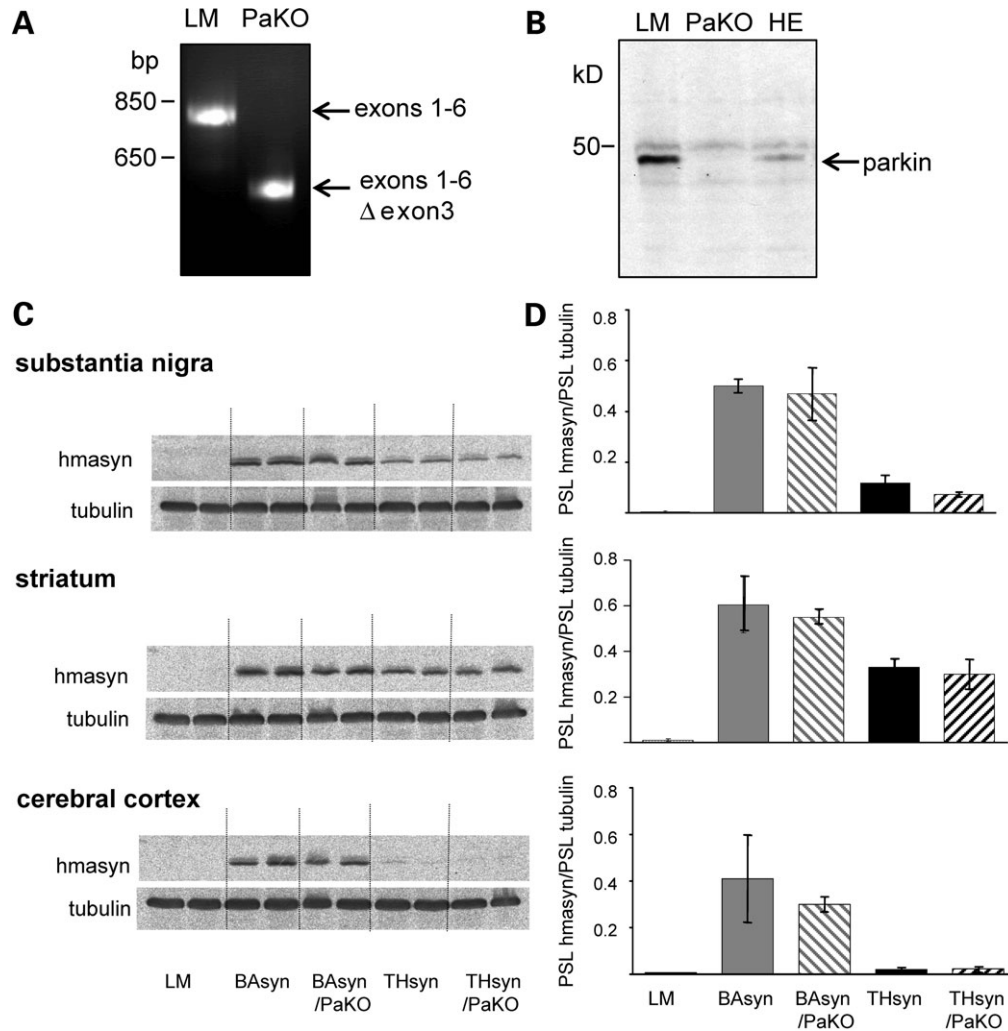


Figure 1. Characterization of transgenic lines. (A) RT-PCR analysis of parkin transcript using primers specific for exons 1 and 6. A 788 bp DNA band in LM brain contains exons 1–6, while a smaller parkin fragment (548 bp) lacks exon 3 in PaKO brain. Subsequent sequencing of the fragment confirmed the exon 3 skipping in parkin transcripts in PaKO brain. (B) Western blot with parkin antibody of total brain proteins from LM, PaKO and HE (heterozygous) mice confirms the reduction of parkin in the HE and the absence of parkin in the PaKO. (C) Comparative analysis of the transgene hm^2 asyn expression in the SN, the ST and the cerebral Cx of mono- and double-mutant transgenic lines. The blots were stripped and probed with an antibody against alpha-tubulin to normalize protein levels. (D) Graph showing quantitative phosphorimager analysis of hm^2 asyn signals (background values subtracted and normalized for protein content) in the different transgenic lines. PSL, photo-stimulated luminescence.

glial cells in order to reduce variations due to possible cell-type specific vulnerabilities to these gene mutations (41) and to differences in antioxidant potential (reviewed in 42).

In all analysed brain regions of old-aged mono- and double-mutant animals, most neurons displayed cytoplasmic vacuoles (Fig. 3A) and a disruption of the Golgi network (Fig. 3B) and the endoplasmic reticulum (Fig. 3C). Occasionally, we observed a detachment of the outer nuclear membrane (Fig. 3C). In addition, neurons displayed a high number of lysosomes and lipofuscin granules (Fig. 3D), which, in contrast to the former pathological features, were also present in similar numbers in LM (control animals) of the same age.

The most prominent feature, however, was abnormal mitochondria. In Figure 3E–I, several examples of mitochondrial changes are shown, including those with electron dense

inclusion bodies (Fig. 3E), dilated and disorganized cristae (Figs 3F–H) and protrusions (Fig. 3I). These mitochondrial alterations were rarely seen in age-matched LM.

To analyse whether dopaminergic neurons also possess these abnormal mitochondria, we used a pre-embedding electron microscopy immunogold technique with an antibody against TH to identify dopaminergic neurons in the SN of aged double-mutants ($n = 2$). Immunogold labelling for TH was primarily seen within neuronal perikarya (Fig. 3J and K) and dendrites. All labelled neuronal somata displayed damaged mitochondria (Fig. 3J) and, in addition, lipofuscin granules (Fig. 3K).

While our observations suggest that the number of damaged mitochondria varies among strains at the age of 12–14 months, we systematically counted these organelles and measured their size in the SN, the ST and the Cx of all mono- and

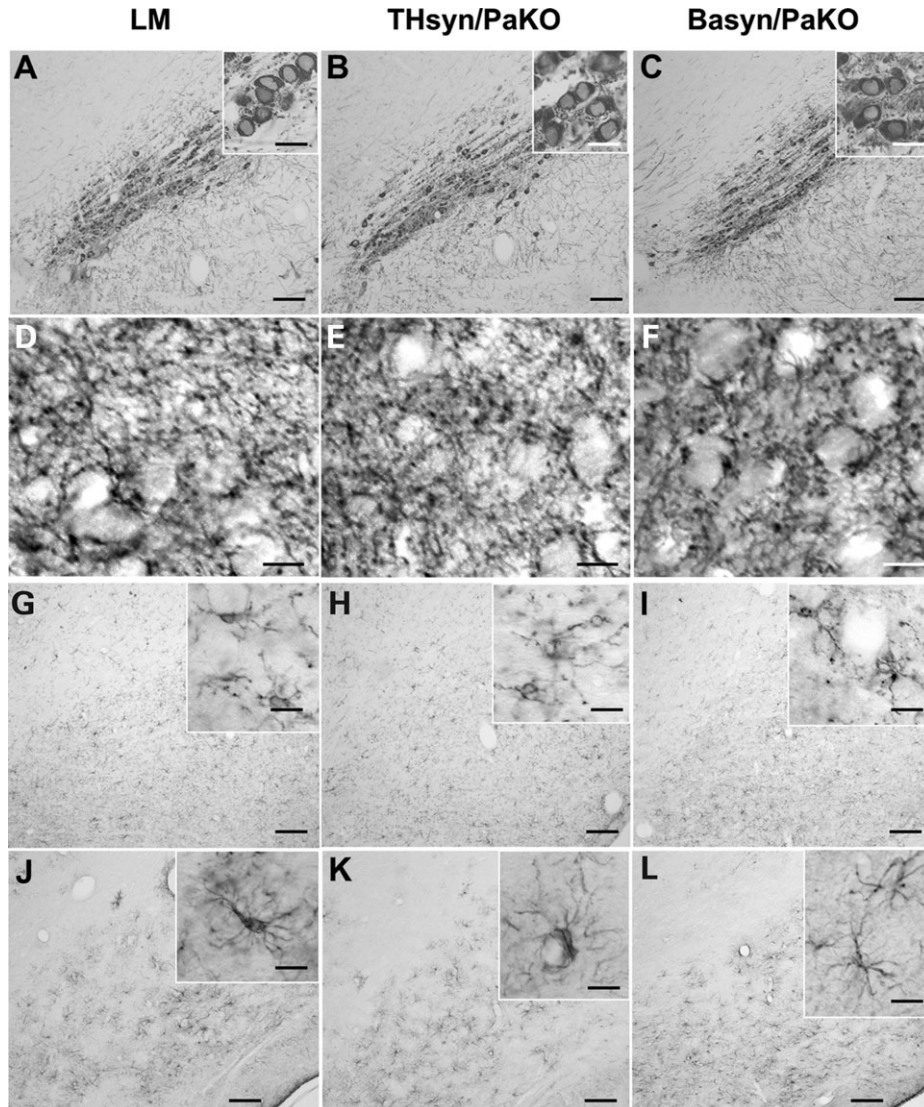


Figure 2. Dopaminergic system, astrocytes and microglia in double-mutant mice, compared with LM. Representative photomicrographs of 12 m old LM, THsyn/PaKO and BASyn/PaKO illustrating TH- (A–F), PT66- (G–I) and GFAP-immunoreactivity (J–L) in the SN (A–C, G–I) and the ST (D–F). No deficits or abnormalities in the number or morphology of immunopositive structures are observed in the double-mutants. Scale bars, 100 μm (A–C, G–I); 25 μm (insets), 10 μm (D–F).

double-mutant animals in comparison with age-matched LM. Of each transgenic line (PaKO, THsyn, BASyn, THsyn/PaKO and BASyn/PaKO) and the LM, four aged animals were analysed. The quantitative ultrastructural analysis confirmed our first impression of an increase in the number of damaged mitochondria in the brain of all transgenic mice (Fig. 4A). Furthermore, our analyses showed that the presence and the number of damaged mitochondria were region- and genotype-dependent. Although in all transgenic (mono- and double-mutant) animals, the number of damaged mitochondria was increased in SN and in some mouse lines also in the Cx, none of the transgenic animals exhibited an increase of damaged mitochondria in the ST when compared with LM. Surprisingly, the extent of mitochondrial alterations also varied among the lines. In the SN, the mean increase of damaged mitochondria was significant ($P < 0.05$) for the

double-mutants (THsyn/PaKO 340%, BASyn/PaKO 195% versus LM) (Fig. 4A), while in the Cx the increase was considerably higher (up to 900% versus LM), but restricted to BASyn and BASyn/PaKO (Fig. 4A). To determine whether these changes in morphology are compensated by a general increase in the number of mitochondria within the affected strains, we counted all mitochondria in the neuronal somata. We generally found higher numbers of this organelle in the SN, but no inter-strain differences within the analysed brain regions (Fig. 4B). Next we analysed mitochondrial swelling to answer the questions whether (i) morphological changes in the affected mice were accompanied by an increase in mitochondrial size and (ii) animals without a significant increase in the number of damaged mitochondria display mitochondrial swelling as an early sign of an emerging structural disorganization. We did not observe mitochondrial swelling in any transgenic line.

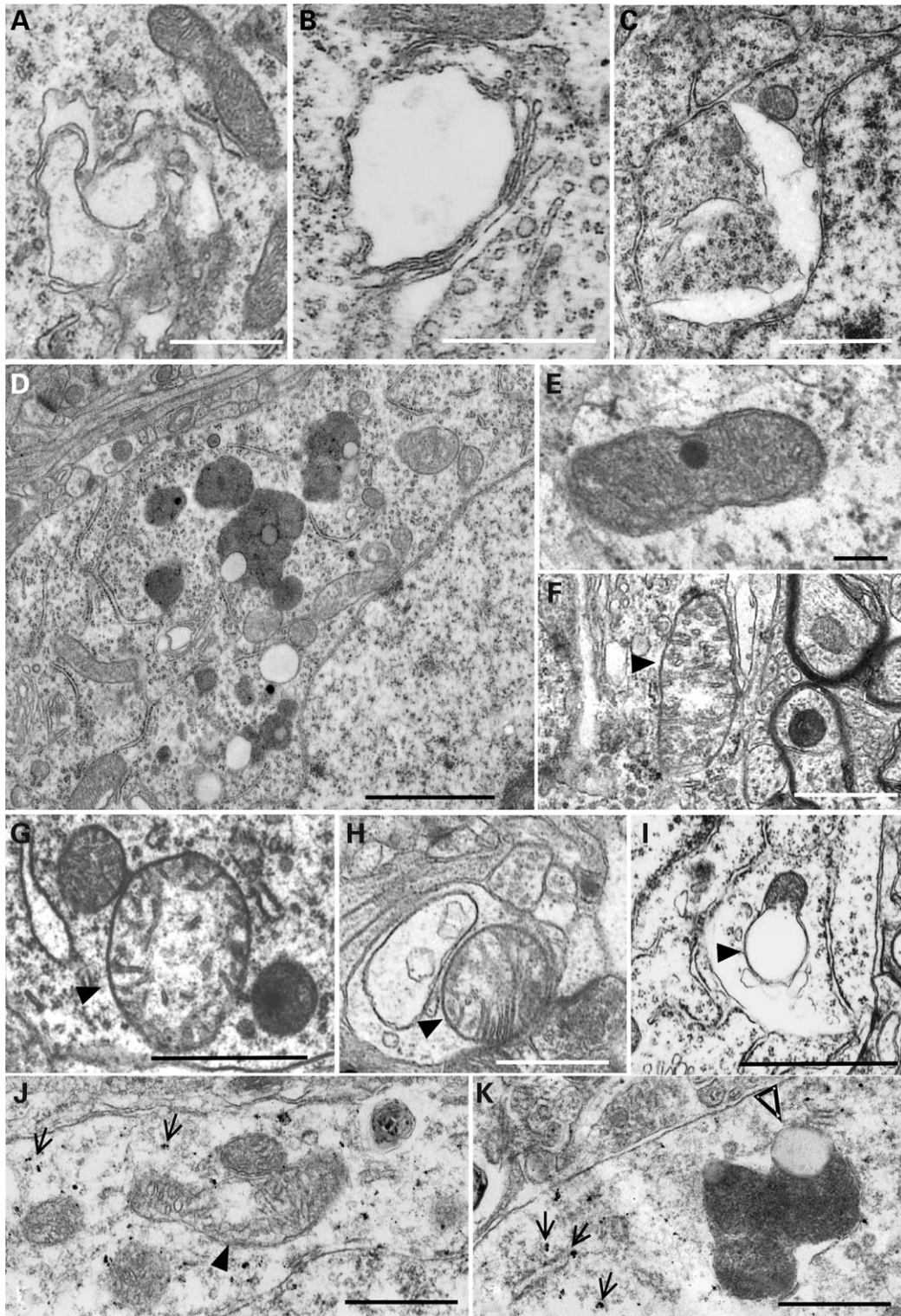


Figure 3. Ultrastructural changes in the brains of double-mutant animals. Electron micrographs of the Cx (A,D–G) and the SN (B,C,H–K) of THsyn/PaKO (B–F,I–K) and BAsyn/PaKO (A,G,H) mice revealed ultrastructural changes in the cytoplasm (A), the Golgi apparatus (B) and the endoplasmic reticulum (C) of neuronal somata. Mitochondria (filled arrowheads) were seriously affected and showed dense inclusion bodies (E), dilated cristae (F–H,J) and protrusions (I). (J,K) Immunogold labelling (small arrows depict gold granules) with TH-antibodies showed that damaged mitochondria (filled arrowhead) and lipofuscin granules (unfilled arrowhead) were also found in dopaminergic neurons. Scale bars, 0.5 μm (A,C,H); 1 μm (B,E,F,G,I–K), 2 μm (D).

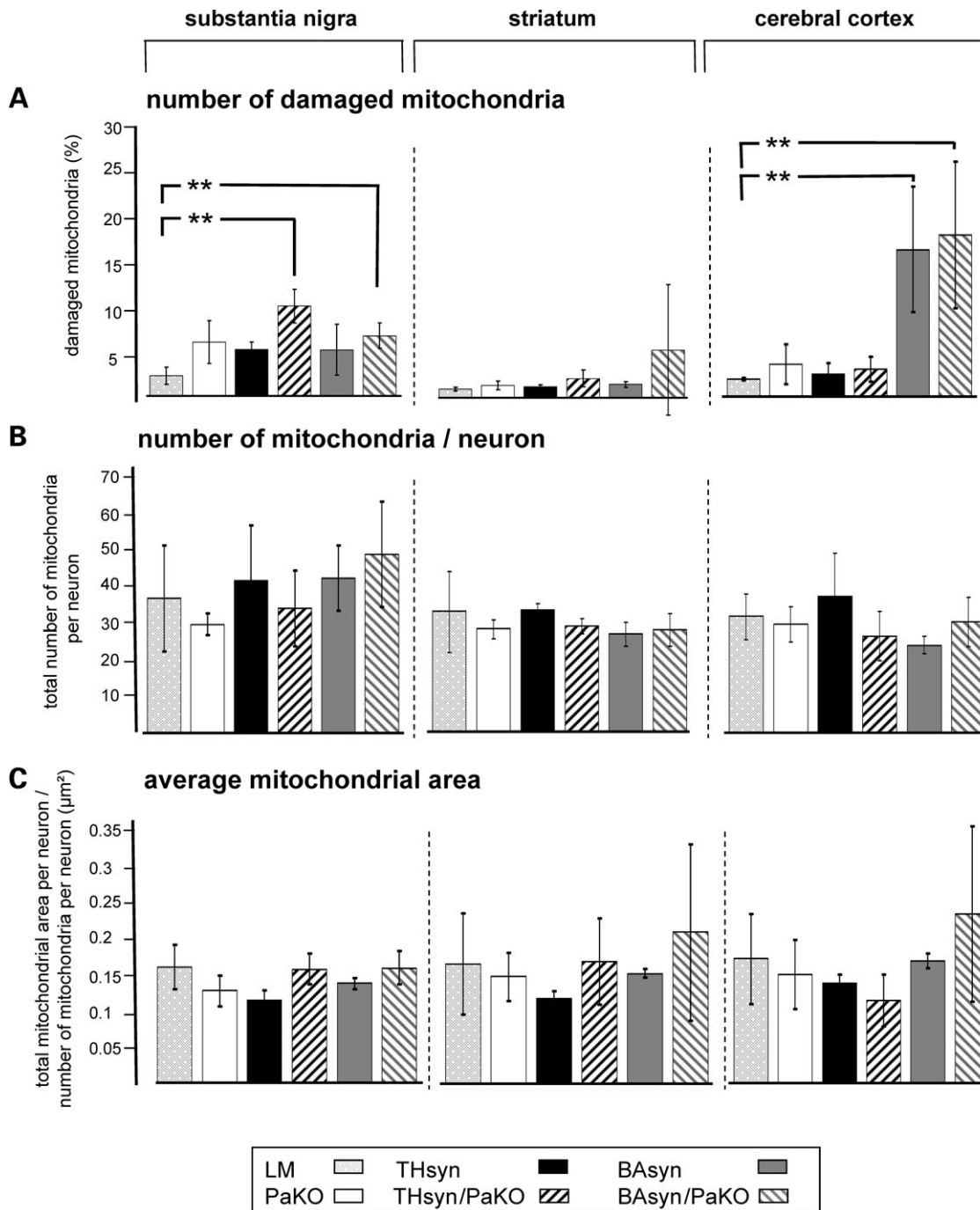


Figure 4. Quantitative analysis of changes in mitochondrial morphology, number and size in the SN, the ST and the Cx of mono- and double-mutant mice at the age of 12–14 m. (A) Graphs showing the percentage of damaged mitochondria in the different brain regions analysed. Compared with LM, significant increases in damaged mitochondria were found in the SN of the double-mutants (THsyn/PaKO and BAyn/PaKO). In the ST, no difference in mitochondrial morphology between transgenic lines and LM were observed, whereas in the Cx the BAyn and BAyn/PaKO exhibited a tremendous increase in damaged mitochondria. (B and C). No change in the total number (B) or the average area of the mitochondria (C) were detected in any analysed brain area. $**P < 0.01$.

Ultrastructure of mitochondria in neurons of young transgenic mice (2–3 months)

Our results suggest the presence of a high number of damaged mitochondria in the SN and the Cx of 12–14 months old mice in some transgenic lines. The gradual progressive nature of PD

in humans raises the question whether the observed changes in the transgenics are also age-related. This would be implicated by the absence or a lower number of damaged mitochondria in early mouse adulthood. To investigate this issue, we analysed the SN and the Cx of 2–3 months old double-mutant animals (THsyn/PaKO and BAyn/PaKO, $n = 4$ for each line).

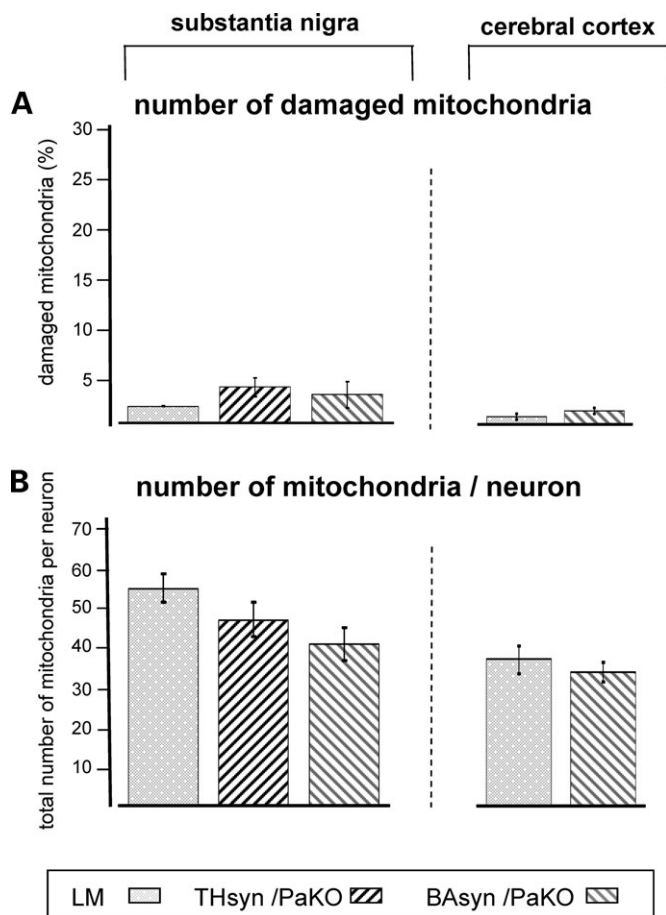


Figure 5. Quantitative analysis of changes in mitochondrial morphology and number in the SN and the Cx of double-mutant mice at the age of 3 m. In 3 m old double-mutants neither the number of damaged mitochondria (A) nor the total number of mitochondria per neuron (B) were increased compared with age-matched LM.

These mouse lines displayed significant mitochondrial damage at old age. As shown in Figure 5, neither the number of damaged mitochondria nor the total number of mitochondria were significantly altered in comparison with age-matched LM. While the number of damaged mitochondria in the LM remained fairly constant with advancing age, our analysis showed that the number increased dramatically in the SN of the double-mutants THsyn/PaKO (3 months 3.3/14 months 9.8) and BAsyn/PaKO (3 months 2.6/14 months 6.5) and in the Cx of BAsyn/PaKO (3 months 2.3/14 months 17.5) (compare Figs 4A and 5A). In addition, in LM and in THsyn/PaKO, the total number of mitochondria decreased with advancing age (e.g. SN: LM 3 months 53/14 months 33, THsyn/PaKO 3 months 45/14 months 31) (compare Figs 4B and 5B), while in BAsyn/PaKO the number remained constant in the Cx (3 months 30/14 months 30) or increased in the SN (3 months 39/14 months 44).

Ultrastructure of mitochondria in skeletal muscles of old transgenic mice (12–14 months)

From histopathological studies of PD patients (35) and of transgenic *Drosophila* models (20,22,36,37), it is evident that

mitochondrial defects are not restricted to neurons but are also present in skeletal muscle. Therefore, we examined mitochondria in skeletal muscle of the double-mutants THsyn/PaKO ($n = 4$) and BAsyn/PaKO ($n = 4$). First, we analysed the expression of the transgene hm²asyn in the skeletal muscle. While the BAsyn/PaKO consistently expressed the transgene, it was neither found in the non-transgenic LM nor in the THsyn/PaKO (Fig. 6A). Ultrastructural microscopy of non-transgenic LM revealed well-organized muscle fibres with many tightly packed normal organized mitochondria (Fig. 6B and C). Some mitochondria, however, appeared hollow and swollen, therefore they were classified as damaged (Fig. 6D). In the double-mutants, mitochondria exhibited the same morphological features. Our quantitative analysis did, however, not reveal a difference in the number of damaged mitochondria between non-transgenic LM and double-mutants (Fig. 6E). However, it was interesting to realize the generally higher number of damaged mitochondria in muscle compared with brain tissues (compare Figs 4A and 6E).

Release of intermembrane space proteins from mitochondria in old transgenic mice (12–14 months)

The levels of cytochrome *c*, Smac/DIABLO and Omi/HtrA2 in the cytosolic and mitochondrial fractions of SN, ST and Cx were determined by western blot analysis. Irrespective of genotype and analysed brain region, the respective proteins were always more prominent in the mitochondrial than the cytosolic fraction. No difference in the ratios of mitochondrial versus cytosolic levels was found in any brain region of the double-mutants compared with age-matched non-transgenic LM (see Supplementary Material, Fig. S1).

Mitochondrial respiration in old transgenic mice (14 months)

Analysis of mitochondria from PD patients demonstrated complex I deficiencies (12,13,15). The morphological changes displayed by mitochondria in our transgenic lines also suggest mitochondrial deficiencies. To address this issue, we examined the respiratory capacity of mitochondria isolated from the brain regions SN, ST and Cx of the various transgenic lines by measuring state 3 and state 4 respiration using substrates for complex I, complex II and complex III/IV. State 3, also termed active respiration, is defined as respiration in the presence of an oxidizable substrate and ADP and thus is a measure of the respiration that is coupled to ATP synthesis. State 4, or resting respiration, is the rate of respiration in the presence of substrate but without ADP, and thus is a measure of the rate of respiration that is not coupled to ATP synthesis. The respiratory control ratio (RCR; ratio of state 3: state 4 respiration) provides a measure of the efficiency of coupling of the electron transport chain and can be used to evaluate the functional intactness of the preparation.

In our study, we performed three series of experiments. In series 1, we measured the mitochondrial respiration rates starting at complexes I, II and III/IV of the SN, ST and Cx of the double-mutant mouse line BAsyn/PaKO and the corresponding monogenics BAsyn and PaKO versus LM.

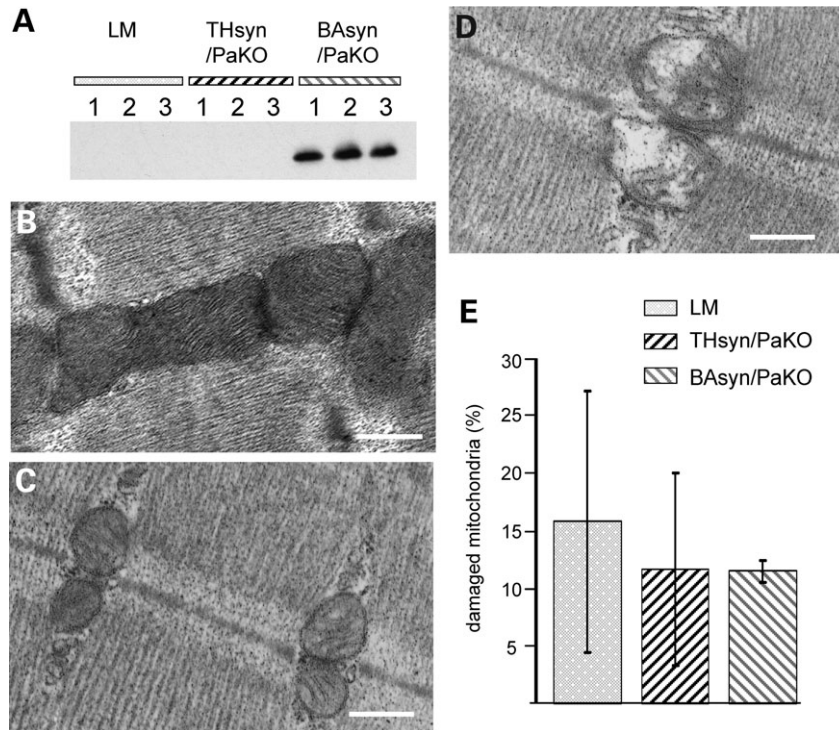


Figure 6. Mitochondria in skeletal muscle of double-mutant animals at the age of 12–14 m. (A) Western blot analysis of the transgene (hm²asyn) expression in skeletal muscle of the LM and the double-mutant lines THsyn/PaKO and BAAsyn/PaKO (1–3, three different animals per line). Only the BAAsyn/PaKO animals expressed the transgene in the skeletal muscle tissue. (B–D) Electron micrographs of muscular mitochondria in LM. Most mitochondria appeared normal (B and C) and only some were swollen with distorted cristae (D). (E) Quantitative analysis of damaged mitochondria in LM, THsyn/PaKO and BAAsyn/PaKO revealed no change in the number of damaged mitochondria in the skeletal muscle. Scale bars, 1 μ m.

In series 2, all respiration rates were analysed in SN and ST of THsyn/PaKO and the monogenics THsyn and PaKO versus LM. In the last series (series 3), we also included an analysis of all respiration rates with/without the uncoupler CCCP (SN, Cx).

Consistent with our morphological data of profound mitochondrial changes in the SN, we observed reduced rates of state 3 respiration starting at the complex I in the SN of the two double-mutant lines BAAsyn/PaKO (series 1: 18.7% reduction, $P < 0.05$) and THsyn/PaKO (series 2: 29.4% reduction, $P < 0.05$; series 3: 21.0% reduction, $P < 0.05$), but not in the monogenics when compared with LM (Fig. 7A), whereas respiratory rates starting at complex II or complex III/IV were unchanged (see Supplementary Material, Table S1), indicating a specific reduction of the complex I activity in the SN of both double-mutants. No significant reduction was observed in state 4 respiration (Fig. 7B) and RCR (Fig. 7C) by using glutamate/malate as substrate. Since state 4 respiration is associated with proton leakage across the inner mitochondrial membrane, the morphological abnormalities observed in the double-mutants may cause the increase of state 4 respiration. To confirm the reduction of complex I function, we measured the respiratory rate in the presence of the uncoupler CCCP, which breaks down the entire proton gradient across the inner mitochondrial membrane. The respiratory rate in THsyn/PaKO was significantly decreased (23.2% reduction, $P < 0.05$) when glutamate/malate was used as substrate after treatment with CCCP (Fig. 7D). The latter assay showed a similar reduction also for PaKO (29.5%

reduction, $P < 0.01$). Complexes II and III/IV in the SN were not affected in any transgenic line (see Supplementary Material, Table S1).

We did not observe a reduction in electron transport chain capacity for any complex in the ST or the Cx of the transgenic lines (see Supplementary Material, Table S1). In view of the serious structural mitochondrial damage in the Cx of BAAsyn/PaKO and BAAsyn, the lack of functional deficits is particularly surprising (Fig. 4A).

DISCUSSION

Studies implicate a diverse array of environmental and genetic factors contributing to the pathophysiology of PD. Increasing lines of evidence suggest that mitochondrial toxicity represents a common target for several if not all of these factors. The goal of the present study was to investigate the pathological effects of PD-associated genes on mitochondrial integrity and function. To address this, we have generated several mono- and double-mutant mouse lines expressing high levels of doubly mutated human asyn (hm²asyn) and/or a targeted deletion of Parkin. Overexpression of human asyn and deletion of the parkin gene were chosen since in humans they are associated with inherited PD as dominant or recessive traits, respectively. In the present study, we have analysed the mitochondrial ultrastructure in various brain regions (SN, ST, Cx) and skeletal muscle of these

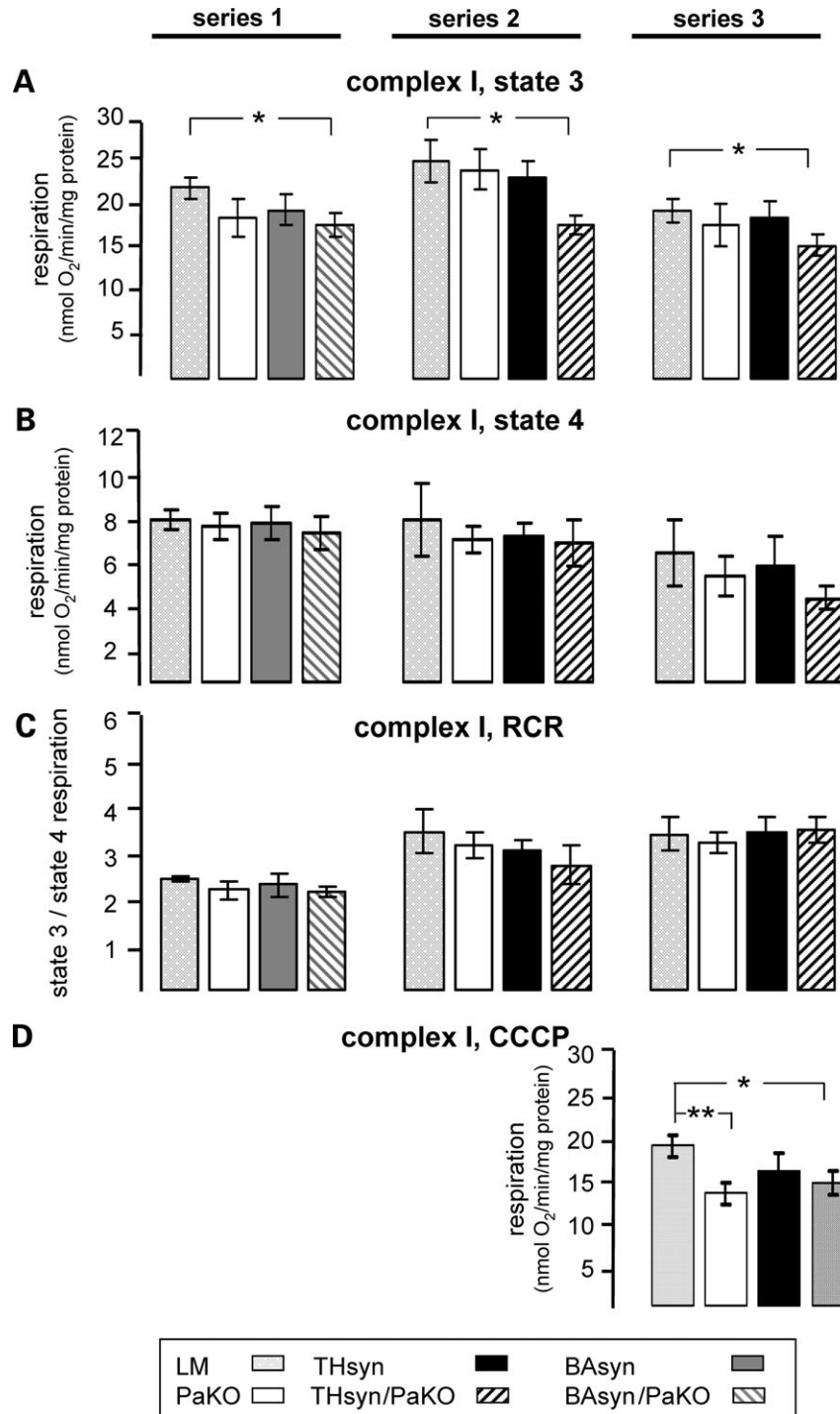


Figure 7. Respiration capacity of complex I in mitochondria of the SN of aged transgenics. Three independent series of measurements with 8–10 animals each were performed (series 1–3) to analyse the respiratory capacity of complex I in LM and the various transgenic lines. Both double-mutant lines, BAAsyn/PaKO (series 1) and THsyn/PaKO (series 2 and 3) showed a significant decrease in state 3 (A) but not in state 4 respiration (B) or the RCR (C). Following treatment with CCCP mitochondria from THsyn/PaKO, but also from PaKO, a significant reduction in uncoupled respiratory rates was observed, indicating a reduced capacity of the electron transport chain (D). **P* < 0.05, ***P* < 0.01. CCCP, carbonyl cyanide *m*-chlorophenoxylhydrazine; RCR, respiratory ratio control.

transgenic mice at young and old age. Moreover, we addressed the question whether the loss of normal mitochondrial architecture is accompanied by the translocation of intermembrane space proteins and/or changes in respiratory capacity.

The main results of this study are severe genotype-, age- and region-dependent morphological alterations of mitochondria in neuronal somata, which are restricted to the brain and lacking in skeletal muscle cells. These alterations are

not accompanied by alterations of the number or the size of the mitochondria or by leakage of cytochrome *c*, Smac/DIABLO or Omi/HtrA2, but in the SN, coincide with a reduced complex I capacity. None of the transgenic animals developed overt motor disabilities or any gross histopathological abnormalities in the analysed brain regions.

General pathology

The main focus of this study was to investigate the effects of PD associated gene mutations on mitochondrial ultrastructure and function. In order to evaluate the mitochondrial alterations in the context of the histopathology of the analysed brain regions, we studied cell death and gliosis as two neuropathological hallmarks of PD. None of the transgenic mouse lines developed a significant histopathological phenotype. We neither observed morphological evidence for damaged neurons nor for gliotic changes in the mesencephalon or the Cx.

Several reports have shown that overexpression of human mutant *asyn* or deletion of Parkin in mice results in variable neuropathological phenotypes. Only some α -synuclein transgenic lines showed morphological alterations in the dopaminergic system (43–45) and all generated Parkin-knockout lines lacked nigral degeneration [parkin-Ex3-Del (46,47); parkin-Ex2-Del (48); parkin-Ex7-Del (45)]. The latter observation is in accordance to our histopathological data. Up to date, only one double-mutant mouse line overexpressing mutant (A53T) human α -synuclein under the control of the prion protein promoter (*prp*) on the background of an exon-7 deleted parkin knockout was reported (49). In accordance with our double-mutants, the double-mutant line generated by von Coelln *et al.* (49) was also indistinguishable from the corresponding monogenics with respect to the expression level of mutated α -synuclein. This result is unexpected since α -synuclein has been shown to be a parkin substrate (50). Moreover, von Coelln *et al.* (49) noted cell death restricted to the brainstem of the double-mutants, which was similar in amount and extent to that observed in the *prp*A53Tsyn transgenics (43). The reasons for this discrepancy in toxic effects between *prp*-driven A53T *hmasyn* and our BA- or TH-driven *hm²asyn* are not clear. Variations in the expression pattern or the level of the transgene might be a reason, but seems to be unlikely since the transgene expression in the BAsyn line does not show considerable regional differences and is remarkably high.

Mitochondrial structure

Although no evidence for cell death has been observed in any of the transgenic mice, we discovered marked alterations in mitochondrial architecture. Subsets of mitochondria appeared swollen, accompanied by disorganized cristae and/or detachment of the outer membrane. These morphological abnormalities observed in some of our transgenic mice bear a striking resemblance to those described in human PD patients (32–35).

It is well established that mitochondria are highly susceptible to morphological artefacts caused by inadequate fixation. Furthermore, fixation by almost any technique is frequently

associated with the presence of at least some swollen and apparently exploded mitochondria, even in tissues which appear to be generally well prepared. However, several arguments led us to the conclusion that the observed changes in this study are not fixation artefacts. First, all animals (controls = LM and transgenes) were fixed in exactly the same way and processed in parallel experiments, but transgenes consistently exhibited more damaged mitochondria than LM. Secondly, we analysed four animals per genotype and age, and every single transgenic animal of a line exhibited a higher number of damaged mitochondria compared with any LM. And finally, the structural variations were significantly lower in young animals and their number depended on the brain region. Altogether, these data argue against a methodological artefact but support an intimate relationship between genetic mutations and structural mitochondrial changes in distinct brain regions.

The most exciting result of our study is the genotype-, age- and region-dependence of the structural mitochondrial changes. In the SN and Cx, all transgenes exhibited an increase in the number of damaged mitochondria. The extent of the increase varied and was significant in the SN for the double-mutants THsyn/PaKO and BAsyn/PaKO, and in the Cx for BAsyn and BAsyn/PaKO. The data implicate that, while both, parkin inactivation and overexpression of *hm²asyn*, induce mitochondrial damage in distinct brain regions, the combination of these mutations induces a much stronger destructive effect on mitochondria. Interestingly, a similar elevation and/or acceleration of pathology by the combination of two disease-associated mutations has been reported for transgenic models of Alzheimer's disease. Although none of the Alzheimer's mouse models completely recapitulates all facets of the disease, the combination of two or even three mutations yielded animals with more lesions and an enhanced progression of the disease than a single mutation (51; reviewed in 52–54). Similarly, in our PD mouse models, the effects of both mutations, parkin inactivation and overexpression of *hm²asyn*, appear to be additive. Consistent with this notion, Parkin and *asyn* have been shown to interact in a common anti-apoptotic cellular pathway (55–57). Moreover, there is evidence that both, Parkin and *asyn*, interact with mitochondrial proteins, supporting the idea that they could indeed converge in a common pathway regulating mitochondrial integrity. Parkin is localized at the outer mitochondrial membrane (18) and associated with the mitochondrial transcription factor A (58), whereas *asyn* exhibits homology to 14-3-3 proteins and is capable to interact with Bad (59). A precise understanding of the complex relationship between Parkin and *asyn* and their influence on mitochondrial structure and function is an important challenge.

The mitochondrial changes in the double-mutants occur with advancing age. In young animals (2–3 months, Fig. 5), mitochondria were morphologically unaltered, but developed severe damage within the following months and were well-established in 12–14-month-old animals (Fig. 4). In recent years, several studies documented that aging itself is associated with changes in number, size, architecture and function of mitochondria (reviewed in 11,60–63), implicating that the observed mitochondrial changes in the old double-mutants might be an age-related effect. However, the higher number

of mitochondria with structural abnormalities observed in our old double-mutants is unlikely to occur as a consequence of aging since age-matched LM did not exhibit similar numbers of such abnormalities. The increase of damaged mitochondria with age may either be related to the age-related decline in compensatory/protective mechanisms or to an interaction of genetic and harmful environmental factors, which accumulate with increasing age. The dynamic nature of the structural changes of mitochondria in double-mutants will potentially render the exploration of the underlying pathophysiological mechanisms possible.

The increase of mitochondrial alterations in the double-mutants was restricted to particular brain regions and absent in skeletal muscle. We show that the double-mutant line THsyn/PaKO developed mitochondrial damage only in the SN, but not in the Cx and the ST, whereas the BAsyn/PaKO line displayed these changes in SN and Cx but not in the ST. Since the Parkin gene is inactivated in every cell of the animals and neurons in PaKO mice do not show increase in structural mitochondrial pathology, the reason for this tissue and region selectivity might either be promoter-induced variations of hm²asyn-expression and/or regional differences in the sensitivity of mitochondria. Evidence for mitochondrial heterogeneity derives from studies analysing biochemical and structural parameters of mitochondria in different CNS regions (64–71). Since comparative studies of the analysed brain regions are missing, the contribution of region-specific features to the differential reactions of the mitochondria cannot be assessed.

Mitochondrial function

Finally, we addressed the question whether the marked increase in the number of structurally altered mitochondria is associated with measurable physiological changes in mitochondrial respiration and/or an enhanced release of the pro-apoptotic proteins cytochrome *c*, Smac/DIABLO and Omi/HtrA2.

We have shown that the structural mitochondrial abnormalities in the SN of double-mutant animals (BAsyn/PaKO and THsyn/PaKO) correlate with a significant decrease (18.7% BAsyn/PaKO/21–29% THsyn/PaKO) in state 3 respiration when glutamate/malate is used as energetic substrate. CCCP treatment, which results in a collapse of the proton gradient across the inner mitochondrial membrane and allows mitochondrial respiration to proceed at maximal capacity, irrespective of the proton leakage, confirmed the reduction of complex I function. State 4 respiration was not reduced. The abnormal mitochondrial morphology in the SN of the double-mutants may cause proton leakage across the inner mitochondrial membrane, thereby increasing the state 4 respiratory rate, and may mask the reduction caused by a deficient function of complex I during the measurement of state 4 respiration.

The changes are similar to functional alterations of complex I described in SN mitochondria of PD patients (12). Interestingly, this decrease in complex I activity is restricted to the SN, even though mitochondria in the Cx of BAsyn and BAsyn/PaKO are also seriously damaged. Other complexes of the respiratory chain are not affected. The regional

selectivity of the functional deficits suggests that dopaminergic neurons are particularly vulnerable. Dopamine and its oxidation products interact with the mitochondrial oxidative phosphorylation system, which may contribute to the inactivation of complex I (72–75). Moreover, a recent study (76) has demonstrated that overexpression of mutant asyn augments the level of catechol species, thereby potentially impairing the oxidative stress situation in dopaminergic neurons. The current observations, however, do not provide sufficient evidence to firmly conclude that the structural damage in mitochondria and the dysfunction of complex I are causally related. Further studies are required to substantiate this assumption or to demonstrate that they are independent pathological features.

In addition to mitochondrial respiration, we analysed the pro-apoptotic intermembrane space proteins cytochrome *c*, Smac/DIABLO and Omi/HtrA2. In light of the structural damage, we expected an enhanced release of these proteins. However, the ratio of mitochondrial and cytosolic amount of these proteins was not changed in any transgenic line. It remains unclear, why the translocation of mitochondrial proteins is not affected, despite the serious damage of mitochondrial structure. One reason may be the relatively low sensitivity of the western blot method, which may not allow the detection of the small variations in cytosolic protein concentrations that can be expected in view of the rather small fraction of damaged mitochondria (7–16%). On the other hand, it is conceivable that the observed disturbance of mitochondrial architecture is not sufficient to release the analysed proteins. Nevertheless, the overt absence of pro-apoptotic factor release might be an explanation for the lack of nigral degeneration in our transgenic mice. To further analyse the functional consequences of the mitochondrial changes, a procedure for the separation of the damaged mitochondria is required.

Together our results provide compelling evidence that (i) α -synuclein and parkin are both relevant for mitochondrial integrity, (ii) the influence of these proteins on mitochondria are age- and tissue-specific and (iii) changes of mitochondrial morphology do not inevitably cause functional impairment.

An inhibition of complex I of the respiratory chain was detected in the SN, but not in other brain regions with similar morphological mitochondrial damage. The fact that there is no pronounced mitochondrial protein release in spite of the remarkable morphological damage visible in mitochondria may explain why even the double-mutants do not develop cell death. Apparently, the observed complex I inhibition in the SN is not sufficient to kill the neurons. It is tempting to speculate that similar mitochondrial damage occurs in humans, and that this species is more prone to severe functional consequences.

MATERIALS AND METHODS

Mouse strains

Five different transgenic lines were analysed in this study: a Parkin-deficient mouse line with a targeted deletion of exon 3 (PaKO); two α -synuclein transgenic lines carrying the doubly mutated human asyn (hm²asyn) driven either by the chicken beta-actin promoter (BAsyn) or by the mouse

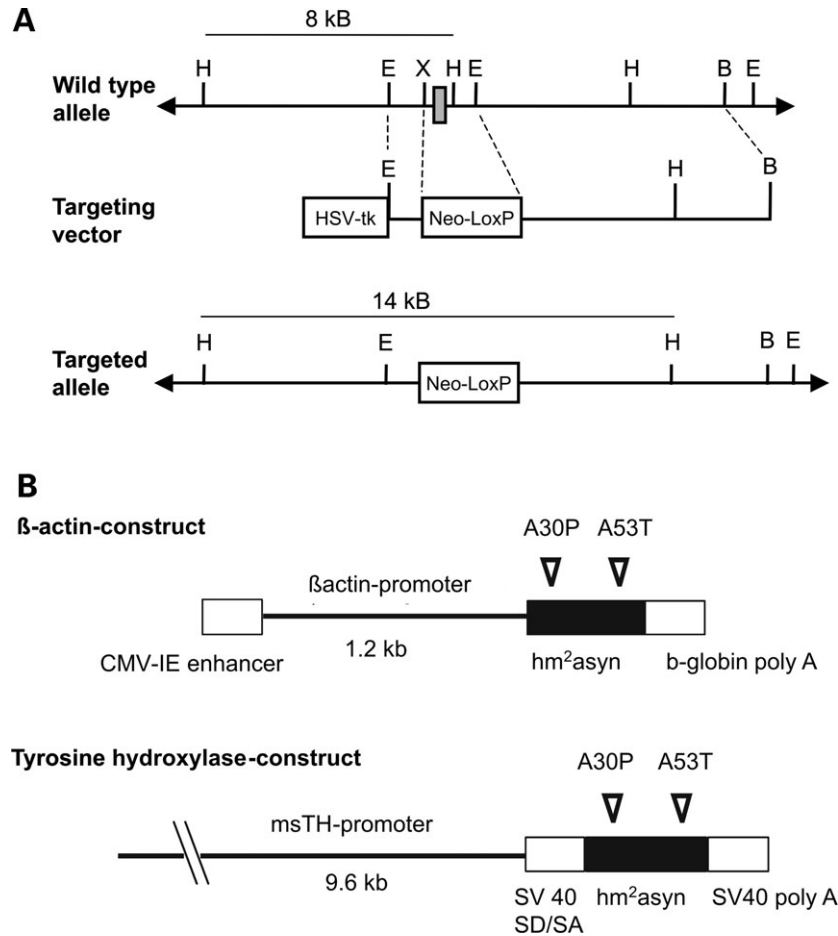


Figure 8. Generation of PaKO and asyn transgenic lines. (A) Strategy for deleting parkin exon 3 (grey box) in the mouse genome. When the targeting construct (middle) recombines homologously with the parkin chromosomal locus (top), a locus is generated (bottom), in which the neomycin resistance cassette flanked with two LoxP elements (Neo-LoxP; open box) has replaced exon 3 of the parkin gene. The external 5'-probe recognizes a 8 kB fragment in *Hind*III-digested wild-type genomic DNA and a 14 kB fragment in targeted genomic DNA. H, *Hind*III; E, *Eco*RI; X, *Xho*I; B, *Bam*HI. (B) Schematic representation of the BA and the TH-construct for the generation of the hm²syn transgenic lines.

tyrosine hydroxylase (TH) promoter (THsyn); two double-mutant lines with a Parkin deletion and the overexpression of hm²asyn driven by the BA- (BA²syn/PaKO) or by the TH-promoter (TH²syn/PaKO), respectively.

For the generation of the PaKO, the 11 kb 129Sv/J mouse genomic DNA fragment containing parkin exon 3 was used to construct a gene targeting vector (Fig. 8A). Three of 500 screened transfected R1 embryonic stem cell clones exhibited the properly targeted parkin allele. One ESC was injected into blastocysts, and yielded male chimeric mice, transmitting the parkin exon 3 deletion to progeny. Heterozygous F1 PaKO mice were intercrossed to generate homozygous PaKO and their LM. The successful deletion was confirmed at the genome level by Southern blotting (data not shown). Offspring were backcrossed into C57BL/6 mice up to the F4-generation, which consequently had a mixed genetic background of C57BL/6 (94%) and 129SvJ (6%).

Transgenic mice expressing the hm²asyn (BA²syn and TH²syn) were generated with the constructs shown in Fig. 8B in a C57BL/6 background as described previously (40,77).

To generate double-mutant lines, we crossed the F4-generation of the PaKO with either BA²syn or TH²syn. The genotypes of the mice were identified by PCR analysis of tail DNA. Control mice were age-matched non-transgenic LM from the same generation of backcrossing. Young (2–3 months) and old mice (12–14 months) were used for the studies.

Immunoblotting

The expression of Parkin and the transgene hm²asyn was evaluated in transgenic mice and age-matched controls by enhanced chemiluminescence (Parkin) or radioactive immunoblotting (hm²asyn). Mice were decapitated and the SN, the ST, the Cx and skeletal muscle were dissected or total brain was frozen in liquid nitrogen. For hm²asyn analysis, tissues were homogenized in homogenization buffer (50 mM HEPES, 150 mM NaCl, 10 mM EDTA, 1% Nonidet P40, 0.5% Na-deoxycholate, 0.1% SDS) containing complete protease inhibitor cocktail (Boehringer Mannheim, Germany) using a Teflon/glass homogenizer at 4°C. After homogenization,

samples were incubated on ice for 30 min, followed by centrifugation for 20 min at 12 000g. The supernatant was collected as cytosolic fraction. For Parkin immunoblotting, tissues were homogenized in sucrose buffer (0.32 M sucrose containing complete protease inhibitor cocktail (Boehringer Mannheim, Germany), centrifuged for 5 min at 1500g, and the supernatant was collected.

For analysis of the release of mitochondrial intermembrane space proteins (cytochrome *c*, Smac/DIABLO, Omi/HtrA2) radioactive immunoblotting was performed from fresh brain tissue (SN, ST, Cx) as described previously (78). Brain tissues were homogenized in homogenization buffer (250 mM sucrose, 10 mM KCl, 1.5 mM MgCl₂, 2 mM EDTA, 20 mM HEPES containing complete protease inhibitor cocktail (Boehringer Mannheim, Germany) using a Teflon/glass homogenizer at 4°C. Homogenized samples were briefly centrifuged for 5 min at 500g, and supernatants were collected and underwent an additional centrifugation for 20 min at 12 000g. The supernatants of this centrifugation were collected as cytosolic fractions, mitochondria were in the pellet.

Protein content was determined with the method of Neuhoff *et al.* (79), after diluting all fractions 1:1 in 2× Laemmli sample buffer and boiling.

For blotting, proteins were separated by electrophoresis on 15% polyacrylamide gels containing 0.1% SDS and transferred with 200 mA for 1.5 h at RT onto a PVDF membrane. Blocking was performed with 3% milk powder and 2% BSA in TBS-Tween (0.1% Tween, 20 mM TBS) at RT for 1 h. Incubation with the primary antisera was performed overnight at 4°C. Antisera were affinity purified rabbit anti-murine Parkin [anti-parkin, 1:10 (80)], mouse anti-human asyn (anti-syn211, 1:2000, Invitrogen, Karlsruhe, Germany), mouse anti-rat cytochrome C (anti-cytC, 1:1000, BD Bioscience, New York, USA), rabbit anti-mouse Smac/DIABLO (second mitochondrial activator of caspases; anti-Smac, 1:2000, ProSci-Incorporated, Poway, USA) and rabbit anti-human Omi/HtrA2 (high temperature requirement protein A2, anti-Omi, 1:1000, Abcam, Cambridge, UK). Subsequently, the blots were washed with TBS-Tween and incubated with either HRP-coupled secondary antibodies, anti-rb (for anti-parkin) (1:10 000, Amersham, München, Germany) and anti-ms (for anti-syn211) (1:50 000, Amersham), or 50 µCi ³⁵S-labeled secondary antibodies anti-ms and anti-rb (Amersham) at RT for 1.5 h. For detection, the membrane was washed three times in TBS-Tween and signals were detected using the ECL-Plus system (Amersham) or the membrane was exposed to a Fuji-Bas imaging plate for 24–48 h and quantified using a PhosphorImager instrument.

To monitor the amount of proteins bound to the blots, they were stripped using Restore™ western Blot Stripping buffer (Pierce, Rockford, IL, USA) according to the manufacturer's recommendations, followed by detection with the antibody mouse anti-chicken alpha-tubulin (1:400 000, Sigma, Taufkirchen, Germany) for testing equal protein loading or with the antibody mouse anti-cow cytochrome *c* oxidase (anti-COX IV, 1:5000, Abcam) to verify mitochondrial purification. Detection was performed as described earlier.

The mean signal intensity of the area of interest (AOI) was corrected for background and protein content (corresponding tubulin band).

Histological stains

To define brain areas, cresyl violet staining was performed according to standard methods. Degenerating neurons were detected using FluoroJadeB-staining as described previously (81).

Immunohistochemistry

Transgenic mice and their age-matched LM were anesthetized by an overdose of a mixture of ketamine (100 mg/kg; Upjohn GmbH, Germany) and rompun (5 mg/kg; Bayer Leverkusen, Germany) and then perfused transcardially with phosphate-buffered saline (PBS) followed by 4% paraformaldehyde (PFA) in 0.1 M phosphate buffer (PB). Brains and skeletal muscle were immediately removed and postfixed in 4% PFA overnight at 4°C. Afterwards, they were either cryoprotected in 30% sterile phosphate-buffered sucrose, frozen in methylbutane between –50 and –70°C and serially cut with a cryostat (40 µm or 10 µm) or embedded in paraffin and serially cut into 18 µm-thick sections.

The expression and localization of TH, the marker for dopaminergic structures, the transgene human asyn (hmasyn), the astrocyte marker glial fibrillary acidic protein (GFAP) and the microglia marker phosphotyrosine (PT66 (82) were examined at the light microscopic level in the SN, the ST and the Cx by means of an immunoperoxidase method with diaminobenzidine as chromogen. Sections stained for TH or GFAP were first cooked for 5 min in 0.01 M citrate buffer (pH 6.0) for antigen retrieval. Following a pre-incubation with 3% normal serum in PBS for 10 min by RT, sections were incubated with one of the primary antibodies: sheep polyclonal antisera anti rat TH (anti-TH, 1:500; Chemicon, Hofheim, Germany), mouse monoclonal antibody specific for hmasyn (anti-syn211, 1:500, Invitrogen), rabbit polyclonal anti cow GFAP (anti-GFAP, 1:250, Acris, Hiddenhausen, Germany) and mouse monoclonal anti PT66 (anti-PT66, 1:1000, Sigma) and then by the corresponding biotinylated secondary antibody, ABC reagent (Axxora, Germany) and silver-gold intensification (83).

Specificity of the immunostainings was tested by pre-incubation with 3% H₂O₂ in methanol to suppress endogenous peroxidase activity and by omission of the primary antibodies.

Transmission electron microscopy

For conventional EM, monogenics, double-mutants and age-matched LM were transcardially perfused with PBS followed by 2% PFA plus 2.5% glutaraldehyde in 0.1 M PB and a post-fixation time of 2 h at 4°C. Sagittal sections, 100 µm thick, were cut with a vibratome, and Cx, ST, SN and skeletal muscle samples were microdissected and placed in 2% OsO₄ for 1 h, dehydrated with graded concentrations of ethanol and Epon-propylene oxide and flat embedded in Epon. Representative ultrathin sections were collected on Formvar-coated grids and contrasted with uranyl acetate and lead citrate.

Immunoelectron microscopy

For pre-embedding electron microscopic immunohistochemistry, animals were transcardially perfused with PBS followed

by 4% PFA plus 0.1% glutaraldehyde in PB and a postfixation overnight. Sagittal sections, 150 μm in thickness, were cut with a Lancer vibratome and then incubated for 2 h in 10 and 20% sucrose/PBS followed by 30% sucrose/PBS overnight. All sections were frozen rapidly over liquid nitrogen and thawed in room temperature PBS to break membranes. For immunohistochemistry, vibratome sections were processed with anti-TH (1:300) for 4 days followed by rb anti-sheep Fab fragments coupled to 1.4 nm gold particles (Biotrend, Germany) diluted 1:100 in PBS plus 10% normal horse serum and 0.2% BSA for 2 h.

After a silver enhancement procedure (Nanoprobes, Yaphank, USA), the SN was dissected, washed and postfixed for 1 h in 2% OsO_4 followed by embedding, cutting and contrasting as described earlier.

Mitochondrial respiration

Mice were decapitated and the SN, the ST and the Cx were rapidly dissected. Corresponding brain regions from the right and left hemisphere were pooled and mitochondria were isolated for each animal and brain region. Tissues were placed into ice-cold isolation medium (0.25 M sucrose, 25 mM HEPES, 1 mM EGTA, 0.2% fatty-acid-free BSA at pH 7.2) and homogenized in a Dounce-type tissue homogenizer. All the following steps were performed at 4°C. The homogenate was centrifuged at 610g for 10 min. The supernatant was removed and centrifuged again at 11 900g for 5 min to obtain the crude mitochondrial pellet. Mitochondria were suspended in isolation medium containing 6.5 mM KH_2PO_4 and protein content was determined by the BCA assay (Pierce, Bonn, Germany).

Three separate series of mitochondrial respiration measurements were performed. In each series, 8–10 animals per genotype were measured. For each animal, brain region and substrate, measurements were performed in triplicates. Mitochondrial respiration was determined in a miniature chamber system (100 μl volume; MT200, Strathkelvin Instr., Glasgow, UK) equipped with a magnetic stirrer and a Clark-type oxygen electrode. Glutamate/malate (8 mM each) (complex I), 4 mM succinate (complex II) or 1 mM ascorbate/0.4 mM N,N,N',N'-tetramethylphenylenediamine (complex III/IV) were used as substrates. State 3 respiration was initiated by the addition of ADP (complex I: 0.35 mM, complex II: 0.23 mM, complex III/IV: 0.12 mM). After ADP depletion, state 4 respiration was measured. After determination of coupled respiration, 0.4 μM carbonyl cyanide *m*-chlorophenoxyhydrazone (CCCP) was added to the reaction chamber and respiration was measured in the absence of a proton gradient. All three respiratory rates were calculated as nmol of O_2 per minute and per milligramme mitochondrial protein and the RCR was calculated as the ratio of the state 3 to the state 4 respiration.

Data analysis

Histology and peroxidase-labelled immunohistochemistry sections were visualized at the microscopic level (Axioskop2; Zeiss, Oberkochen, Germany) under brightfield illumination and Nomarski optics. Structures were described according to the main subdivisions of the brain and were identified with the

aid of the atlas of Paxinos and Franklin (84). The anatomic terminology used in this study is based on this atlas. Images were captured with an imaging system (JVC, KY-F75U camera) connected to a computer equipped with an image program (Diskus 4.50, Hilgers, Königswinter, Germany). For final output, images were processed using Photoimpact 4 software.

Ultrathin sections were visualized using a Phillips EM-410 electron microscope. The morphology, number and size of mitochondria in brain were evaluated in digitized electron microscopy images of three different brain regions of 2–3 months and 12–14 months old transgenic and LM animals. In total, 20 neuronal somata per brain region (cerebral Cx—primary motor Cx layers I–VI; SN—pars compacta and reticulata; ST) taken from two different vibratome sections (100 μm thick) of each animal were independently analysed by two examiners blind with regard to the genotype, the brain region and the age of the animals. Ultrathin sections were selected at random from the middle of the vibratome sections to avoid potential structural irregularities that might occur on the surface of the vibratome sections. Neurons were counted only if they contained a nucleus surrounded by cytoplasm. Of each transgenic line (PaKO, THsyn, BAsyn, THsyn/PaKO and BAsyn/PaKO) and the LM, four animals per age group were analysed. Morphological changes of muscle mitochondria were evaluated in skeletal muscle specimen from double-mutants (THsyn/PaKO and BAsyn/PaKO, $n = 3$) and LM ($n = 3$) at the age of 12–14 months. In total, several pictures per muscle taken from 2–3 vibratome sections (100 μm thick) of each animal were examined in a blinded fashion.

Mitochondria were classified as structurally damaged when one or more of the following alterations were observed: distorted or disrupted cristae, detachment of the outer membrane or protrusions from the outer membrane (see Figs 3 and 6). The area of mitochondria, lysosomes, nuclei and somata were measured using the image program Diskus 4.50 (Hilgers, Königswinter, Germany). Data are presented as mean \pm SD of the means of the four analysed animals per genotype.

Statistical analysis of ultrastructural changes was carried out using one-way analysis of variance followed by the *post hoc* Tukey test when significance (at the $P < 0.05$ level) was indicated. If tests on normality and equal variances failed, an *H*-test was performed. In all cases, the null hypothesis was rejected at the $P < 0.05$ level. When comparisons were made between two genotypes, a Student's *t*-test was performed and $P < 0.05$ was considered significant. To avoid accumulation of α -errors in multiple *t*-tests, *P*-values were adjusted with the Bonferroni-method.

Data of mitochondrial respiration are presented as mean \pm SE. For comparison with the control group (LM), the Student's *t*-test was employed. Statistical significance was assumed at $P < 0.05$.

ACKNOWLEDGEMENTS

The authors thank Petra Jergolla, Katja Schmidtke, Renate Scholl, Katrin Schuster and Holger Schlierenkamp for excellent technical assistance.

Conflict of Interest statement. None declared.

REFERENCES

- Ramirez, A., Heimbach, A., Grundemann, J., Stiller, B., Hampshire, D., Cid, L.P., Goebel, I., Mubaidin, A.F., Wriekat, A.L., Roeper, J. *et al.* (2006) Hereditary parkinsonism with dementia is caused by mutations in ATP13A2, encoding a lysosomal type 5 P-type ATPase. *Nat. Genet.*, **38**, 1184–1191.
- Mizuno, Y., Hattori, N., Yoshino, H., Hatano, Y., Satoh, K., Tomiyama, H. and Li, Y. (2006) Progress in familial Parkinson's disease. *J. Neural Transm. Suppl.*, 191–204.
- Klein, C. and Schlossmacher, M.G. (2006) The genetics of Parkinson disease: implications for neurological care. *Nat. Clin. Pract. Neurol.*, **2**, 136–146.
- Schapira, A.H. (2006) Etiology of Parkinson's disease. *Neurology*, **66**, S10–S23.
- Dekker, M.C., Bonifati, V. and Van Duijn, C.M. (2003) Parkinson's disease: piecing together a genetic jigsaw. *Brain*, **126**, 1722–1733.
- Mori, H., Kondo, T., Yokochi, M., Matsumine, H., Nakagawa-Hattori, Y., Miyake, T., Suda, K. and Mizuno, Y. (1998) Pathologic and biochemical studies of juvenile parkinsonism linked to chromosome 6q. *Neurology*, **51**, 890–892.
- Takahashi, H., Ohama, E., Suzuki, S., Horikawa, Y., Ishikawa, A., Morita, T., Tsuji, S. and Ikuta, F. (1994) Familial juvenile parkinsonism: clinical and pathological study in a family. *Neurology*, **44**, 437–441.
- Abou-Sleiman, P.M., Muqit, M.M. and Wood, N.W. (2006) Expanding insights of mitochondrial dysfunction in Parkinson's disease. *Nat. Rev. Neurosci.*, **7**, 207–219.
- Wersinger, C. and Sidhu, A. (2006) An inflammatory pathomechanism for Parkinson's disease? *Curr. Med. Chem.*, **13**, 591–602.
- Moore, D.J., West, A.B., Dawson, V.L. and Dawson, T.M. (2005) Molecular pathophysiology of Parkinson's disease. *Annu. Rev. Neurosci.*, **28**, 57–87.
- Lin, M.T. and Beal, M.F. (2006) Mitochondrial dysfunction and oxidative stress in neurodegenerative diseases. *Nature*, **443**, 787–795.
- Schapira, A.H., Cooper, J.M., Dexter, D., Jenner, P., Clark, J.B. and Marsden, C.D. (1989) Mitochondrial complex I deficiency in Parkinson's disease. *Lancet*, **1**, 1269.
- Mizuno, Y., Ohta, S., Tanaka, M., Takamiya, S., Suzuki, K., Sato, T., Oya, H., Ozawa, T. and Kagawa, Y. (1989) Deficiencies in complex I subunits of the respiratory chain in Parkinson's disease. *Biochem. Biophys. Res. Commun.*, **163**, 1450–1455.
- Keeney, P.M., Xie, J., Capaldi, R.A. and Bennett, J.P., Jr. (2006) Parkinson's disease brain mitochondrial complex I has oxidatively damaged subunits and is functionally impaired and misassembled. *J. Neurosci.*, **26**, 5256–5264.
- Parker, W.D., Jr., Boyson, S.J. and Parks, J.K. (1989) Abnormalities of the electron transport chain in idiopathic Parkinson's disease. *Ann. Neurol.*, **26**, 719–723.
- Muftuoglu, M., Elilib, B., Dalmizrak, O., Ercan, A., Kulaksiz, G., Ogun, H., Dalkara, T. and Ozer, N. (2004) Mitochondrial complex I and IV activities in leukocytes from patients with parkin mutations. *Mov. Disord.*, **19**, 544–548.
- Zhang, L., Shimoji, M., Thomas, B., Moore, D.J., Torp, R., Ottersen, O.P., Dawson, T.M. and Dawson, V.L. (2004) Mitochondrial localization of the Parkinson's disease related gene DJ-1: implications for pathogenesis. *Hum. Mol. Genet.*, **14**, 2063–2073.
- Darios, F., Corti, O., Lucking, C.B., Hampe, C., Muriel, M.P., Abbas, N., Gu, W.J., Hirsch, E.C., Rooney, T., Ruberg, M. and Brice, A. (2003) Parkin prevents mitochondrial swelling and cytochrome c release in mitochondria-dependent cell death. *Hum. Mol. Genet.*, **12**, 517–526.
- Canet-Aviles, R.M., Wilson, M.A., Miller, D.W., Ahmad, R., McLendon, C., Bandyopadhyay, S., Baptista, M.J., Ringe, D., Petsko, G.A. and Cookson, M.R. (2004) The Parkinson's disease protein DJ-1 is neuroprotective due to cysteine-sulfenic acid-driven mitochondrial localization. *Proc. Natl Acad. Sci. USA*, **101**, 9103–9108.
- Clark, I.E., Dodson, M.W., Jiang, C., Cao, J.H., Huh, J.R., Seol, J.H., Yoo, S.J., Hay, B.A. and Guo, M. (2006) *Drosophila* pink1 is required for mitochondrial function and interacts genetically with parkin. *Nature*, **441**, 1162–1166.
- Martins, L.M., Morrison, A., Klupsch, K., Fedele, V., Moiso, N., Teismann, P., Abuin, A., Grau, E., Geppert, M., Livi, G.P. *et al.* (2004) Neuroprotective role of the Reaper-related serine protease HtrA2/Omi revealed by targeted deletion in mice. *Mol. Cell Biol.*, **24**, 9848–9862.
- Park, J., Lee, S.B., Lee, S., Kim, Y., Song, S., Kim, S., Bae, E., Kim, J., Shong, M., Kim, J.M. and Chung, J. (2006) Mitochondrial dysfunction in *Drosophila* PINK1 mutants is complemented by parkin. *Nature*, **441**, 1157–1161.
- Song, D.D., Shults, C.W., Sisk, A., Rockenstein, E. and Masliah, E. (2004) Enhanced substantia nigra mitochondrial pathology in human alpha-synuclein transgenic mice after treatment with MPTP. *Exp. Neurol.*, **186**, 158–172.
- Richfield, E.K., Thiruchelvam, M.J., Cory-Slechta, D.A., Wuertzer, C., Gainetdinov, R.R., Caron, M.G., Di Monte, D.A. and Federoff, H.J. (2002) Behavioral and neurochemical effects of wild-type and mutated human alpha-synuclein in transgenic mice. *Exp. Neurol.*, **175**, 35–48.
- Pesah, Y., Pham, T., Burgess, H., Middlebrooks, B., Verstreken, P., Zhou, Y., Harding, M., Bellen, H. and Mardon, G. (2004) *Drosophila* parkin mutants have decreased mass and cell size and increased sensitivity to oxygen radical stress. *Development*, **131**, 2183–2194.
- Kim, R.H., Smith, P.D., Aleyasin, H., Hayley, S., Mount, M.P., Pownall, S., Wakeham, A., You, T., Kalia, S.K., Horne, P. *et al.* (2005) Hypersensitivity of DJ-1-deficient mice to 1-methyl-4-phenyl-1,2,3,6-tetrahydropyridine (MPTP) and oxidative stress. *Proc. Natl Acad. Sci. USA*, **102**, 5215–5220.
- Ellis, C.E., Murphy, E.J., Mitchell, D.C., Golovko, M.Y., Scaglia, F., Barcelo-Coblijn, G.C. and Nussbaum, R.L. (2005) Mitochondrial lipid abnormality and electron transport chain impairment in mice lacking alpha-synuclein. *Mol. Cell Biol.*, **25**, 10190–10201.
- Martin, L.J., Pan, Y., Proce, A.C., Aterling, W., Copeland, N.G., Jenkins, N.A., Price, D.L. and Lee, M.K. (2006) Parkinson's disease alpha-synuclein transgenic mice develop neuronal mitochondrial degeneration and cell death. *J. Neurosci.*, **26**, 41–50.
- Palacino, J.J., Sagi, D., Goldberg, M.S., Krauss, S., Motz, C., Wacker, M., Klose, J. and Shen, J. (2004) Mitochondrial dysfunction and oxidative damage in parkin-deficient mice. *J. Biol. Chem.*, **279**, 18614–18622.
- Periquet, M., Corti, O., Jacquier, S. and Brice, A. (2005) Proteomic analysis of parkin knockout mice: alterations in energy metabolism, protein handling and synaptic function. *J. Neurochem.*, **95**, 1259–1276.
- Poon, H.F., Frasier, M., Shreve, N., Calabrese, V., Wolozin, B. and Butterfield, D.A. (2005) Mitochondrial associated metabolic proteins are selectively oxidized in A30P alpha-synuclein transgenic mice—a model of familial Parkinson's disease. *Neurobiol. Dis.*, **18**, 492–498.
- de Mattos, J.P., Alencar, A., da Silva, A.G. and Fonseca, M.E. (1989) Ultrastructural aspects of Parkinson disease. *Arq Neuropsiquiatr.*, **47**, 430–437.
- Trimmer, P.A., Swerdlow, R.H., Parks, J.K., Keeney, P., Bennett, J.P., Jr., Miller, S.W., Davis, R.E. and Parker, W.D., Jr. (2000) Abnormal mitochondrial morphology in sporadic Parkinson's and Alzheimer's disease cybrid cell lines. *Exp. Neurol.*, **162**, 37–50.
- Hayashida, K., Oyanagi, S., Mizutani, Y. and Yokochi, M. (1993) An early cytoplasmic change before Lewy body maturation: an ultrastructural study of the substantia nigra from an autopsy case of juvenile parkinsonism. *Acta Neuropathol. (Berl.)*, **85**, 445–448.
- Winkler-Stuck, K., Kirches, E., Mawrin, C., Dietzmann, K., Lins, H., Wallesch, C.W., Kunz, W.S. and Wiedemann, F.R. (2005) Re-evaluation of the dysfunction of mitochondrial respiratory chain in skeletal muscle of patients with Parkinson's disease. *J. Neural Transm.*, **112**, 499–518.
- Yang, Y., Gehrke, S., Imai, Y., Huang, Z., Ouyang, Y., Wang, J.W., Yang, L., Beal, M.F., Vogel, H. and Lu, B. (2006) Mitochondrial pathology and muscle and dopaminergic neuron degeneration caused by inactivation of *Drosophila* Pink1 is rescued by Parkin. *Proc. Natl Acad. Sci. USA*, **103**, 10793–10798.
- Greene, J.C., Whitworth, A.J., Kuo, I., Andrews, L.A., Feany, M.B. and Pallanck, L.J. (2003) Mitochondrial pathology and apoptotic muscle degeneration in *Drosophila* parkin mutants. *Proc. Natl Acad. Sci. USA*, **100**, 4078–4083.
- Bader, V., Zhu, X.R., Lücking, C.B. and Stichel, C.C. (2006) Mitochondrial pathology in bigenic mouse models of Parkinson's disease. *FENS Abstr.*, **3**, A057.3.
- Kitada, T., Asakawa, S., Hattori, N., Matsumine, H., Yamamura, Y., Minoshima, S., Yokochi, M., Mizuno, Y. and Shimizu, N. (1998)

- Mutations in the parkin gene cause autosomal recessive juvenile parkinsonism. *Nature*, **392**, 605–608.
40. Maskri, L., Zhu, X.R., Fritzen, S., Kühn, K., Ullmer, C., Engels, P., Andriske, M., Stichel, C.C. and Lübbert, H. (2004) Influence of different promoters on the expression pattern of mutated human alpha-synuclein in transgenic mice. *Neurodegen. Disease*, **1**, 255–265.
 41. Ledesma, M.D., Galvan, C., Hellias, B., Dotti, C. and Jensen, P.H. (2002) Astrocytic but not neuronal increased expression and redistribution of parkin during unfolded protein stress. *J. Neurochem.*, **83**, 1431–1440.
 42. Dringen, R., Pawlowski, P.G. and Hirrlinger, J. (2005) Peroxide detoxification by brain cells. *J. Neurosci. Res.*, **79**, 157–165.
 43. Lee, M.K., Stirling, W., Xu, Y., Xu, X., Qui, D., Mandir, A.S., Dawson, T.M., Copeland, N.G., Jenkins, N.A. and Price, D.L. (2002) Human alpha-synuclein-harboring familial Parkinson's disease-linked Ala-53 → Thr mutation causes neurodegenerative disease with alpha-synuclein aggregation in transgenic mice. *Proc. Natl Acad. Sci. USA*, **99**, 8968–8973.
 44. Masliah, E., Rockenstein, E., Veinbergs, I., Mallory, M., Hashimoto, M., Takeda, A., Sagara, Y., Sisk, A. and Mucke, L. (2000) Dopaminergic loss and inclusion body formation in alpha-synuclein mice: implications for neurodegenerative disorders. *Science*, **287**, 1265–1269.
 45. von Coelln, R., Thomas, B., Savitt, J.M., Lim, K.L., Sasaki, M., Hess, E.J., Dawson, V.L. and Dawson, T.M. (2004) Loss of locus coeruleus neurons and reduced startle in parkin null mice. *Proc. Natl Acad. Sci. USA*, **101**, 10744–10749.
 46. Itier, J.M., Ibanez, P., Mena, M.A., Abbas, N., Cohen-Salmon, C., Bohme, G.A., Laville, M., Pratt, J., Corti, O., Pradier, L. *et al.* (2003) Parkin gene inactivation alters behaviour and dopamine neurotransmission in the mouse. *Hum. Mol. Genet.*, **12**, 2277–2291.
 47. Goldberg, M.S., Fleming, S.M., Palacino, J.J., Cepeda, C., Lam, H.A., Bhatnagar, A., Meloni, E.G., Wu, N., Ackerson, L.C., Klapstein, G.J. *et al.* (2003) Parkin-deficient mice exhibit nigrostriatal deficits but not loss of dopaminergic neurons. *J. Biol. Chem.*, **278**, 43628–43635.
 48. Perez, F.A. and Palmiter, R.D. (2005) Parkin-deficient mice are not a robust model of parkinsonism. *Proc. Natl Acad. Sci. USA*, **102**, 2174–2179.
 49. von Coelln, R., Thomas, B., Andrabi, S.A., Lim, K.L., Savitt, J.M., Saffary, R., Stirling, W., Bruno, K., Hess, E.J., Lee, M.K. *et al.* (2006) Inclusion body formation and neurodegeneration are parkin independent in a mouse model of alpha-synucleinopathy. *J. Neurosci.*, **26**, 3685–3696.
 50. Shimura, H., Schlossmacher, M.G., Hattori, N., Frosch, M.P., Trockenbacher, A., Schneider, R., Mizuno, Y., Kosik, K.S. and Selkoe, D.J. (2001) Ubiquitination of a new form of a-synuclein by parkin from human brain: implications for Parkinson's disease. *Science*, **293**, 263–269.
 51. Oddo, S., Caccamo, A., Shepherd, J.D., Murphy, M.P., Golde, T.E., Kaye, R., Metherate, R., Mattson, M.P., Akbari, Y. and LaFerla, F.M. (2003) Triple-transgenic model of Alzheimer's disease with plaques and tangles: intracellular Abeta and synaptic dysfunction. *Neuron*, **39**, 409–421.
 52. Spire, T.L. and Hyman, B.T. (2005) Transgenic models of Alzheimer's disease: learning from animals. *NeuroRx*, **2**, 423–437.
 53. McGowan, E., Eriksen, J. and Hutton, M. (2006) A decade of modeling Alzheimer's disease in transgenic mice. *Trends Genet.*, **22**, 281–289.
 54. Janus, C., Chishti, M.A. and Westaway, D. (2000) Transgenic mouse models of Alzheimer's disease. *Biochem. Biophys. Acta*, **1502**, 63–75.
 55. Machida, Y., Chiba, T., Takayanagi, A., Tanaka, Y., Asanuma, M., Ogawa, N., Koyama, A., Iwatsubo, T., Ito, S., Jansen, P.H. *et al.* (2005) Common anti-apoptotic roles of parkin and alpha-synuclein in human dopaminergic cells. *Biochem. Biophys. Res. Commun.*, **332**, 233–240.
 56. Lo, B.C., Schneider, B.L., Bauer, M., Sajadi, A., Brice, A., Iwatsubo, T. and Aebischer, P. (2004) Lentiviral vector delivery of parkin prevents dopaminergic degeneration in an alpha-synuclein rat model of Parkinson's disease. *Proc. Natl Acad. Sci. USA*, **101**, 17510–17515.
 57. Petrucelli, L., O'Farrell, C., Lockhart, P.J., Baptista, M., Kehoe, K., Vink, L., Choi, P., Wolozin, B., Farrer, M., Hardy, J. and Cookson, M.R. (2002) Parkin protects against the toxicity associated with mutant alpha-synuclein: proteasome dysfunction selectively affects catecholaminergic neurons. *Neuron*, **36**, 1007–1019.
 58. Kuroda, Y., Mitsui, T., Kunishige, M., Shono, M., Akaike, M., Azuma, H. and Matsumoto, T. (2006) Parkin enhances mitochondrial biogenesis in proliferating cells. *Hum. Mol. Genet.*, **15**, 883–895.
 59. Ostrerova, N., Petrucelli, L., Farrer, M., Mehta, N., Choi, P., Hardy, J. and Wolozin, B. (1999) a-synuclein shares physical and functional homology with 14-3-3 proteins. *J. Neurosci.*, **19**, 5782–5791.
 60. Brunk, U.T. and Terman, A. (2002) The mitochondrial-lysosomal axis theory of aging: accumulation of damaged mitochondria as a result of imperfect autophagocytosis. *Eur. J. Biochem.*, **269**, 1996–2002.
 61. Bertoni-Freddari, C., Fattoretti, P., Giorgetti, B., Solazzi, M., Balietti, M. and Meier-Ruge, W. (2004) Role of mitochondrial deterioration in physiological and pathological brain aging. *Gerontology*, **50**, 187–192.
 62. Aoun, P., Simpkins, J.W. and Agarwal, N. (2003) Role of PPAR-gamma ligands in neuroprotection against glutamate-induced cytotoxicity in retinal ganglion cells. *Invest. Ophthalmol. Vis. Sci.*, **44**, 2999–3004.
 63. Toescu, E.C., Myronova, N. and Verkhratsky, A. (2000) Age-related structural and functional changes of brain mitochondria. *Cell Calcium*, **28**, 329–338.
 64. Sullivan, P.G., Rabchevsky, A.G., Keller, J.N., Lovell, M., Sodhi, A., Hart, R.P. and Scheff, S.W. (2004) Intrinsic differences in brain and spinal cord mitochondria: Implication for therapeutic interventions. *J. Comp. Neurol.*, **474**, 524–534.
 65. Friberg, H., Connern, C., Halestrap, A.P. and Wieloch, T. (1999) Differences in the activation of the mitochondrial permeability transition among brain regions in the rat correlate with selective vulnerability. *J. Neurochem.*, **72**, 2488–2497.
 66. Lai, J.C. (1992) Oxidative metabolism in neuronal and non-neuronal mitochondria. *Can. J. Physiol. Pharmacol.*, **70** (suppl.), S130–S137.
 67. Brustovetsky, N., Brustovetsky, T., Purl, K.J., Capano, M., Crompton, M. and Dubinsky, J.M. (2003) Increased susceptibility of striatal mitochondria to calcium-induced permeability transition. *J. Neurosci.*, **23**, 4858–4867.
 68. Battino, M., Bertoli, E., Formiggini, G., Sassi, S., Gorini, A., Villa, R.F. and Lenaz, G. (1991) Structural and functional aspects of the respiratory chain of synaptic and nonsynaptic mitochondria derived from selected brain regions. *J. Bioenerg. Biomembr.*, **23**, 345–363.
 69. Lai, J.C., Leung, T.K. and Lim, L. (1994) Heterogeneity of monoamine oxidase activities in synaptic and non-synaptic mitochondria derived from three brain regions: some functional implications. *Metab. Brain Dis.*, **9**, 53–66.
 70. Collins, T.J., Berridge, M.J., Lipp, P. and Bootman, M.D. (2002) Mitochondria are morphologically and functionally heterogeneous within cells. *EMBO J.*, **21**, 1616–1627.
 71. Liang, C.L., Wang, T.T., Luby-Phelps, K. and German, D.C. (2007) Mitochondria mass is low in mouse substantia nigra dopamine neurons: Implications for Parkinson's disease. *Exp. Neurol.*, **203**, 370–380.
 72. Berman, S.B. and Hastings, T.G. (1999) Dopamine oxidation alters mitochondrial respiration and induces permeability transition in brain mitochondria: implications for Parkinson's disease. *J. Neurochem.*, **73**, 1127–1137.
 73. Gluck, M.R. and Zeevalk, G.D. (2004) Inhibition of brain mitochondrial respiration by dopamine and its metabolites: implications for Parkinson's disease and catecholamine-associated diseases. *J. Neurochem.*, **91**, 788–795.
 74. Ben-Shachar, D., Zuk, R., Gazawi, H. and Ljubuncic, P. (2004) Dopamine toxicity involves mitochondrial complex I inhibition: implications to dopamine-related neuropsychiatric disorders. *Biochem. Pharmacol.*, **67**, 1965–1974.
 75. Khan, F.H., Sen, T., Maiti, A.K., Jana, S., Chatterjee, U. and Chakrabarti, S. (2005) Inhibition of rat brain mitochondrial electron transport chain activity by dopamine oxidation products during extended *in vitro* incubation: implications for Parkinson's disease. *Biochim. Biophys. Acta*, **1741**, 65–74.
 76. Mosharov, E.V., Staal, R.G., Bove, J., Prou, D., Hananiya, A., Markov, D., Poulsen, N., Larsen, K.E., Moore, C.M., Troyer, M.D. *et al.* (2006) Alpha-synuclein overexpression increases cytosolic catecholamine concentration. *J. Neurosci.*, **26**, 9304–9311.
 77. Schoenebeck, B., Bader, V., Zhu, X.R., Schmitz, B., Lübbert, H. and Stichel, C.C. (2005) Sgk1, a cell survival response, in neurodegenerative diseases. *Mol. Cell. Neurosci.*, **30**, 249–264.
 78. Guegan, C., Vila, M., Rosoklija, G., Hays, A.P. and Przedborski, S. (2001) Recruitment of the mitochondrial-dependent apoptotic pathway in amyotrophic lateral sclerosis. *J. Neurosci.*, **21**, 6569–6576.
 79. Neuhoff, V.P.K., Zimmer, H.G. and Mesecke, S. (1979) A simple and versatile, sensitive and volume-independent method for quantitative

- protein determination with independence of other external influences. *Hoppe-Seyler's Z. Physiol. Chem.*, **360**, 1657–1670.
80. Stichel, C.C., Augustin, M., Kuhn, K., Zhu, X.R., Engels, P., Ullmer, C. and Lubbert, H. (2000) Parkin expression in the adult mouse brain. *Eur. J. Neurosci.*, **12**, 4181–4194.
81. Kühn, K., Wellen, J., Link, N., Maskri, L., Lübbert, H. and Stichel, C.C. (2003) The mouse MPTP model: gene expression changes in dopaminergic neurons. *Eur. J. Neurosci.*, **1**, 1–12.
82. Tillotson, M.L. and Wood, J.G. (1989) Phosphotyrosine antibodies specifically label amoeboid microglia *in vitro* and ramified microglia *in vivo*. *Glia*, **2**, 412–419.
83. Stichel, C.C., Singer, W. and Zilles, K. (1990) Ultrastructure of PkC(II/III)-immunopositive structures in rat primary visual cortex. *Exp. Brain Res.*, **82**, 575–584.
84. Paxinos, G. and Franklin, K.B.J. (2001) *The Mouse Brain in Stereotaxic Coordinates*. Academic Press, San Diego.